JOURNAL OF APPLIED ELECTROCHEMISTRY 20 (1990) 786–792

Electrochemically formed transient ReS_2/Re_2O_7 heterojunction with high energy conversion efficiency

B. SCHUBERT, H. TRIBUTSCH

Hahn-Meitner-Institut (Berlin), Abt. Solare Energetik, Glienicker Strasse 100, 1000 Berlin 39, F.R.G.

Received 31 August 1989; revised 12 December 1989

During electrochemical oxidation of ReS_2 crystals the anodic photocurrent in aqueous electrolytes increases up to 140-fold. This phenomenon is accompanied by the formation of an unstable Re_2O_7 surface layer and a characteristic change of the photocurrent spectrum in the near UV. This is explained in terms of the formation of a heterojunction between ReS_2 and Re_2O_7. Upon addition of the I^-/I_3^- redox couple a temporarily working electrochemical solar cell is obtained. Since the observed quantum efficiency exceeded the theoretical expectation, further studies of the interfacial quantum processes were made. It turned out that the enhancement effect is due to light collection by scattering processes in the highly refractive Re_2O_7 film and at the epoxy insulation.

1. Introduction

Rhenium compounds, especially rhenium oxides, have long been used as highly selective catalysts for various chemical mechanisms. Among these it is worth mentioning the hydrocracking of middle fraction oils to naphtha, carbonyl reduction in the presence of carbon double bonds, and many additional hydrogenation reactions [1–3]. In spite of such practical interest, Re_2O_7 has apparently received little attention with respect to its electrochemical and interfacial behaviour, probably due to its hygroscopic properties.

ReO_2 and ReS_2 have been studied as electrodes in electrochemical cells [4–6]. Rhenium disulfide is a semiconductor with an energy gap of 1.33 eV [7] which exists both as a p- and n-type material. Besides cyclic photocurrent voltage studies, flatband potential measurements and photocurrent spectra have been provided [6,5].

We became interested in the (photo)catalytic properties of ReS_2, which contains an Re_4-cluster. During research on (photo)electrocatalysis at such interfaces, which will be reported elsewhere [8], an interesting interfacial phenomenon was encountered which is reported in this contribution.

2. Material

2.1. *Structure*

ReS_2 is layer-type semiconductor (van der Waals gap: 0.6 nm) with triclinic symmetry, space group $P\bar{1}$ [9]. ReS_2 is thus extremely anisotropic. The structure of ReS_2 can be considered as a distorted $CdCl_2$ structure. The layers in Fig. 1a run parallel to the (ab) level. As a consequence of the small bonding distances (0.265 nm, Fig. 1a), the metal atoms build Re_4 clusters. For comparison, in Re metal the bond distance between the Re-atoms is 0.275 nm [10]. These Re_4-clusters line up in the b-direction to form chains. The Re–Re interaction splits the d bands into a filled valence band and an empty conduction band. The Re–Re interaction also involves a change in the translation symmetry, which thus results in a distortion of the $CdCl_2$ structure. ReS_2 has been shown to be a semiconductor with a band-gap of 1.33 eV [7]; the activation energy at room temperature is 0.2 eV [9]. In layer-type semiconductors, the conductivity perpendicular to the layers is often lower by a factor of 100 than within the layers ($\rho_{perp} = 1000\,\Omega$cm at room temperature [9]).

The structure of Re_2O_7 [11] is shown in Fig. 1b. Re_2O_7 is also layer-structured, with a 0.73 nm thick double layer. These double layers have only van der Waals contacts to their neighbours. Since Re_2O_7 occurs as $(Re_2O_7)_2$ units, diamagnetism is to be expected and semiconducting behaviour is also possible. In pure form, Re_2O_7 appears to be an insulator with a band-gap of 2.6 eV [12, 13].

2.2. *Synthesis*

Previously Juza and Biltz [14] described ReS_2 synthesis from elemental Re and S. The disulphide is by far the most stable phase within the Re–S-system ($\Delta G_f^0 = 200\,kJ\,mol^{-1}$ at room temperature [15]). Wildervanck and Jellinek [9] succeeded in preparing the first single crystals by chemical vapour transport. Chemical transport with iodine produced *p*-ReS_2 crystals [6], and transport with bromine resulted in *n*-ReS_2 crystals [5].

2.3. *Preparation of n-ReS_2 single crystals in a chlorine atmosphere*

A quartz tube (22 mm wide) was etched with HF, rinsed with distilled water, annealed in a vacuum and

0021-891X/90 $03.00 + .12

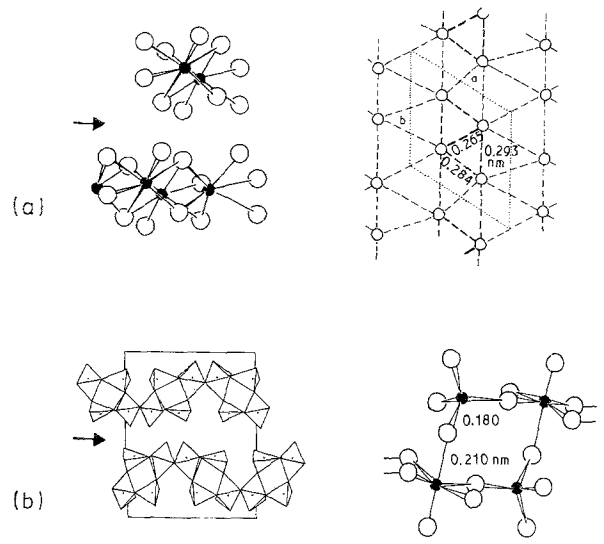

Fig. 1. (a) Left: structure of ReS_2 (filled circles: Re) showing the van der Waals gap (arrow) [30]; Right: illustration of the Re-clusters forming chains [23]; (b) left: structure of Re_2O_7 [11] (dots: Re); right: one more detailed $(Re_2O_7)_2$-unit.

loaded with 1 g Re (Ventron m5N). To remove the oxides from the surface, it was reduced several times with H_2 at 800° C (10 min each time). Subsequently a stoichiometric quantity of sulphur (Ventron m6N) was added, and in vacuum about 10 g Cl_2 condensed by cooling with liquid N_2. The ampoule was sealed at about 10^{-5} Torr and heated to 450/650° C in a two-zone furnace for several days. The product of complete reaction was a fine black powder. For the transport reaction, this powder was heated to 1080/1100° C. The crystals thus prepared had a surface area up to 6 mm^2 but were only 60 nm thick. Recrystallization at 1040/1060° C produced thicker (1–5 μm) black crystals of up to 2 mm^2. These thicker crystals show remarkably good current voltage characteristics in different electrolytes. The following measurements and discussions refer to these thicker crystals unless otherwise noted.

X-ray powder diffraction patterns of the product are the same as for the known bromine-transported ReS_2 (ASTM-card 27-502 [16]).

3. Experimental details

3.1. *Crystal-mounting*

The biggest ReS_2 crystals with the cleanest surface were selected under the microscope to be used for the electrode preparation. They had an average size of 0.3–1.5 mm^2. The crystals were attached onto Vespel-insulated copper shafts with silver epoxy (3M, 105). After dehydration at 40° C, the crystals were 'etched' with scotch tape and encapsulated with epoxy resin (Scotch cast 3M, XR 5241). This was done with utmost case and only the surfaces appearing optically perfect were left blank. The active crystal surface was thus considerably reduced – partially to less than 0.05 mm^2.

3.2. *Recording conditions*

A standard photoelectrochemical set-up was used for current–voltage measurements (potentiostat: Bank POS 73, chopper: PAR 9479, light source. Leitz W-Hal 250 W, XY-recorder: Rhode & Schwarz, ZSK2). A saturated calomel electrode (SCE) was used as the reference electrode and a platinum ring electrode served as the counter electrode. A salt bridge protected the electrolyte against the KCl of the calomel electrode. A water containing tank served as an IR filter to protect the specimen against excessive heating. The light intensity upon the specimen was adjusted to $\sim 100\,mW\,cm^{-2}$. The current–voltage curves were recorded in a N_2 saturated solution unless otherwise indicated.

For recording the photocurrent spectra the following components were used: light source (Oriel, W-halogen 250W); chopper (PAR, 9479); monochromator (Kratos GM 252); potentiostat (HEKA, 28P06); lock-in amplifier (EG & G PAR, 124 A). All photocurrent spectra were recorded with a chopper frequency of 70 Hz. Optical filters were used to eliminate the second harmonics.

3.3. *Size determination*

The size of the electrodes was determined by (1) taking 20–80 fold enlarged Polaroid pictures and (2) comparing the weights of two transparent foils; one homologous to the shape of the crystal on the pictures, the other of a given size.

4. Results

4.1. *Photoelectrochemical characterization*

Across a $ReS_2/0.5\,M\,K_2SO_4$ interface, in the absence of illumination and in the range of -1 to $+2.8$ V with respect to SCE, a very small current flows (less than $10\,\mu A\,cm^{-2}$). This current does not increase during cycling in the absence of light. Under illumination the photocurrent remains below $1\,mA\,cm^{-2}$ during the first cycle. By subsequent cyclic voltamograms the height of this photocurrent increases up to 140 times (Fig. 2). This photocurrent-amplification factor varies with different crystals between 10 and 140. After an anodic passage of charge of $\sim 50\,C\,cm^{-2}$ the photocurrent maintains its level and will thus be called 'stabilized-photocurrent' (henceforth referred to as I_{ph}^{S}). I_{ph}^{S} indicates the difference between the upper solid curve (I_{light}) and the dashed curve (I_{dark}) (see Fig. 2). This anodic charge passage under light involves also a slight increase of the dark current.

Immediately after stabilization of an electrode in $0.5\,M\,K_2SO_4$, two new peaks appear: a reduction peak and an oxidation peak (see Fig. 3). The photocurrent curve here corresponds to the I_{ph}^{S} in Fig. 2. Figure 3 clearly indicates that these two peaks increase with the number of cycles. Subsequent measurements

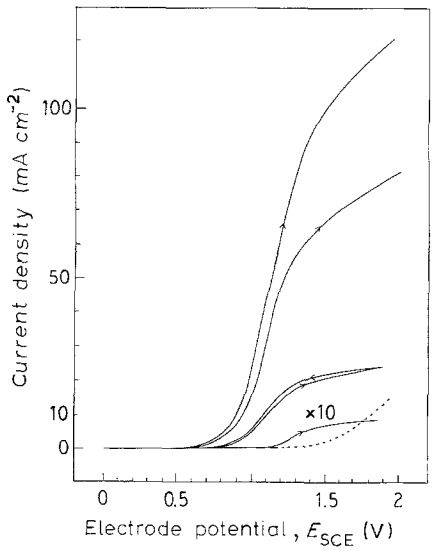

Fig. 2. Stabilization of ReS_2 in 0.5 M K_2SO_4 by anodic polarization under illumination. Scan: 100 mV s^{-1}. Charge passed per sweep: 100–200 mC cm^{-2}. The highest solid curve is obtained after roughly 50 C cm^{-2} have passed; the corresponding dark current for this curve is shown as dashed curve.

showed that these two peaks belong to the same redox-reaction.

Photoelectrochemical experiments made in O_2 saturated solutions showed similar effects. However, the photocurrent stabilization is achieved already after 1 C cm^{-2} instead of 50 C cm^{-2}.

Figure 4 indicates current voltage characteristics of ReS_2 in various electrolytes after stabilization in the respective electrolyte. The effect of photocurrent enhancement is particularly obvious in K_2SO_4 and KCl, less distinctive in KBr, and practically not present in KI.

In Fig. 5, the current is plotted as a function of time under comparable electrochemical conditions in the presence and absence of light in 1 M KCl at +1.5 V: phase I describes the stabilization; point A indicates that I_{ph}^{S} is achieved (the cyclic voltamograms demonstrate that simultaneously two additional peaks appear, see above). Phase II (0.5–5 h at +1.5 V) indicates

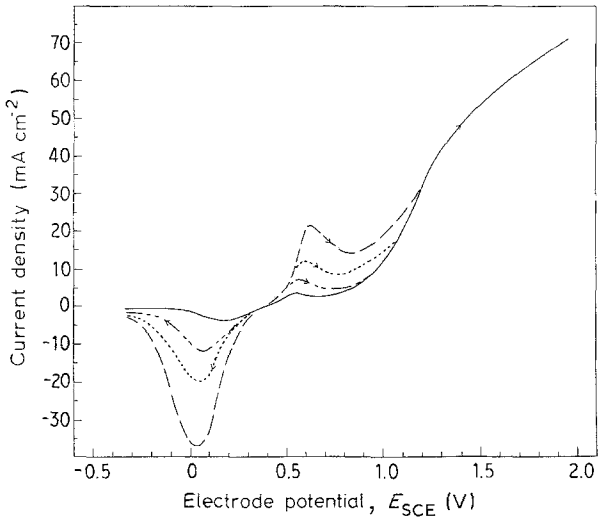

Fig. 3. Cyclic voltamograms of ReS_2 in 0.5 M K_2SO_4 after stabilization. The sequence is: solid, dashed, dotted, dash-dotted; Scan: 100 mV s^{-1}.

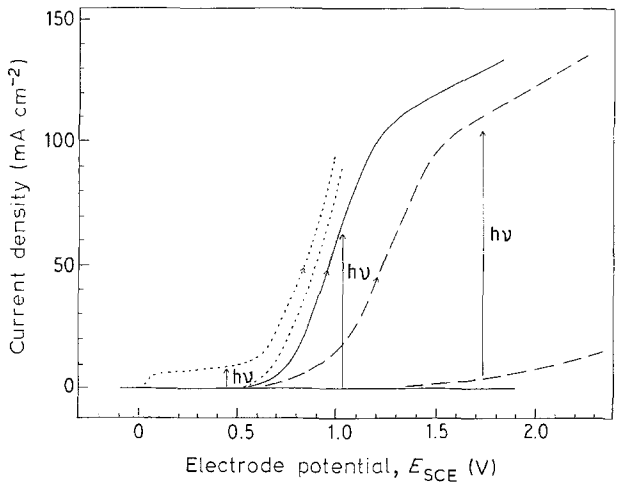

Fig. 4. Current-voltage characteristic of ReS_2 in various electrolytes after being stabilized in these electrolytes: 1 M KI (dotted), 0.5 M K_2SO_4 (solid) and 1 M KCl (dashed).

practically no change of the photocurrent after stabilization. Phase III indicates a constant decrease of the photocurrent and a simultaneous increase of the dark current. In KCl (Fig. 5), after 16 h the crystal is corroded. Comparable ReS_2 crystals corrode in K_2SO_4 after 11 h, while in KI the much smaller photocurrent disappears after about 22 h without achieving a complete corrosion of the crystal.

The above mentioned effect of stabilization is also reflected in the photocurrent spectra: a continuous anodic passage of charge leads to a continuous increase of the photocurrents but also the shape of the spectra changes (see Fig. 6). It should be noted that for a better demonstration of the change in the shape the curves were normalized to the same photocurrent value at 2.2 eV. Summarizing, it can be said that continuous anodic passage of charge causes an increase of the photocurrent, which is higher around 3.3 eV than it is in the low-energy region.

4.2. *Highly efficient transient photoelectrochemical junction*

When ReS_2 is placed in contact with an aqueous solution containing KI, a photovoltage of 340 mV and a

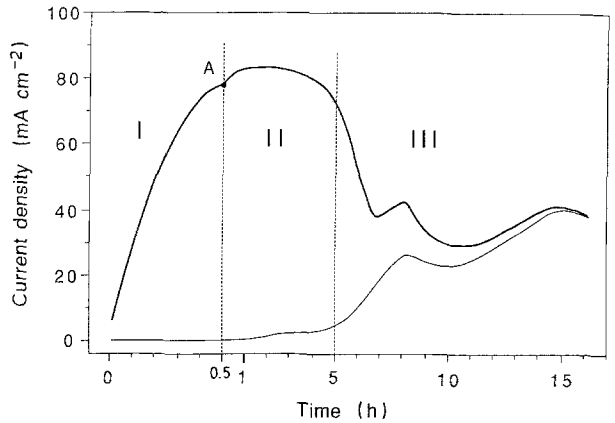

Fig. 5. Time dependent current flow with (solid) and without light (dashed) in 0.5 M K_2SO_4 at +1.7 V.

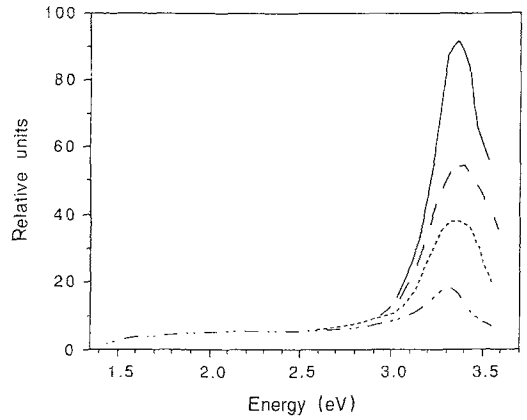

Fig. 6. Photocurrent spectra of ReS_2 in 0.5 M K_2SO_4; the anodic charge flow rises as indicated: dashed, dotted, solid.

photocurrent curve with a fill factor of 0.47 is observed which gives an energy efficiency of $\eta = 1.3\%$ (Fig. 4). This efficiency could be considerably increased if one would succed (1) in stabilizing an electrode in K_2SO_4 or KCl and (2) in maintaining the thus obtained efficient junction in a subsequent measurement in KI. The respective tests were made and yielded positive results (Fig. 7): Immediately after I_{ph}^S in 0.5 M K_2SO_4 is achieved, the subsequent measurement in KI indicates a proportional increase of the photocurrent and no steep rise of I_{dark} above 0.6 V is observed. Approximately 1 min later the characteristic has changed back to the normal situation: a continuous steep rise of I_{dark} positive of 0.6 V and a lower photocurrent are observed in KI without stabilization.

At AM1 and having a semiconductor with a band gap of 1.33 eV, a photocurrent of 34 mA cm^{-2} is theoretically expected [17]. Figure 5, however, suggests a quantum efficiency of about 3 and an energy conversion efficiency of 15% (photovoltage: 400 mV, fill factor: 0.37). These contradictions will be resolved in the discussion, where it will be shown that we are dealing with a light collection phenomena (see Fig. 10). It is interesting that the same electrode can be restabilized in 0.5 M K_2SO_4 and thus makes repeated tests possible.

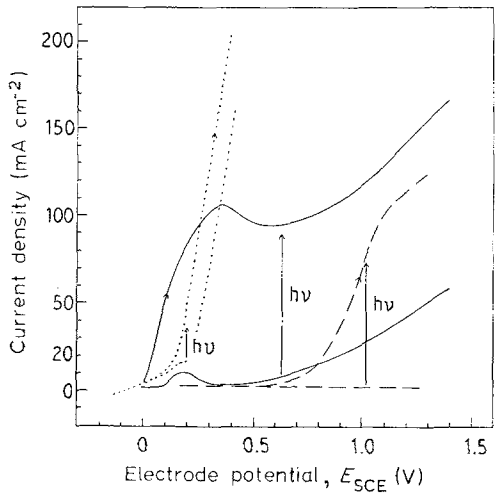

Fig. 7. Current-voltage characteristic of ReS_2 after stabilization in 0.5 M K_2SO_4 (dashed), immediately afterwards in about 1 M KI (dotted), about 1 min later in 1 M KI (solid).

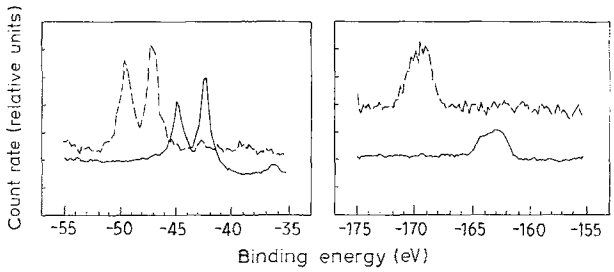

Fig. 8. Relevant details (left: Re_{4f} states, right: S_{2p} states) from the XPS-Spectrum before (solid) and after (dashed) oxidation of ReS_2 (by air, 80° C, several hours).

4.3. *Photoelectronspectroscopy*

A pure surface of the ReS_2 was obtained by splitting the specimens in the UHV. Details of the XPS-spectrum are shown in Fig. 8. Exposure of the specimen to air (80° C) for some hours involves shifts of the S and Re related peaks (Fig. 8, dashed peaks): The Re_{4f}-level appears now at −46.9 eV and thus clearly indicates Re_2O_7 [18] while the S_{2p}-level appears at −169.2 eV and thus indicates sulphate [19]. Since the depth of electron emission is 2–5 nm deep (MgK_α, information depth is ~5 nm) the layer thickness is likewise assumed to exceed 5 nm. This result is supported by other measurements and reflects the corrosion sensitivity of the material.

5. Discussion

At *n*-type ReS_2 in contact with K_2SO_4 high anodic photocurrents are measured. The light-produced positive charge carriers are consumed by oxidation reactions. Since rhenium disulphide undergoes relatively quick corrosion and no O_2 evolution could be detected, these holes form rhenium oxides of higher oxidation states and sulphate. Oxides that may occur are ReO_2, Re_2O_5, ReO_3, and Re_2O_7 [20]. Re_2O_5 can be excluded because it cannot be maintained under the given conditions [21, 22].

The question as to which kind of oxide is formed is first studied by analyzing the changes in the photocurrent spectra (Fig. 6): In the visible area, the spectra are as expected — the band gap amounts to 1.37 eV (indirect), the shape proves to be analogous to the corresponding absorption spectrum [23]. However, the increase of the photocurrent at photon energies > 2.6 eV is striking. Assuming that the oxide in question is not metallic (E_G about 2.6 eV) then energies > E_G are able to create electron-hole pairs in the oxide which may contribute to the rise of the photocurrent in this area.

ReO_2 and ReO_3 are metallic species while Re_2O_7 is reported to be an insulator [12, 13]. It is further known that all dry oxidations of Re compounds result in the formation of the stable Re_2O_7 [18, 20], which is supported by our XPS measurements with ReS_2 (Fig. 8). In an aqueous solution ReO_4^- is formed by oxidation, i.e., oxidation state VII is also reached [20, 24]. So, it can be concluded that probably Re_2O_7

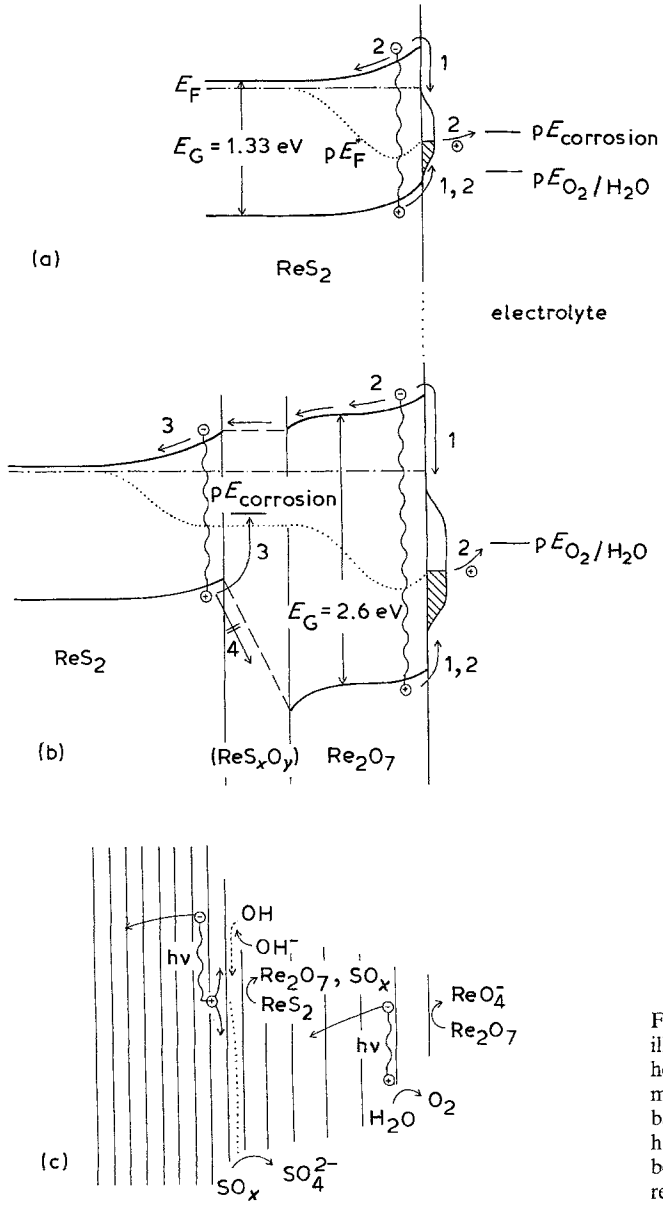

Fig. 9. (a) Energetic scheme of the ReS_2/electrolyte-interface under illumination (with surface states); (b) energetic scheme of the heterojunction ReS_2/Re_2O_7. The area ReO_xS_y suggests that transmutation may be a gradual process. Exact level of the Re_2O_7 bands is not known, but they cannot be so negative that the holes can move to the surface (arrow 4), because of the purely *n*-type behaviour of the cascade-system. (c) illustration of the corrosion reaction in K_2SO_4 containing solution.

is formed on ReS_2 during electrochemical oxidation, thus forming a ReS_2/Re_2O_7 heterojunction. To support the formation of Re_2O_7 on top of ReS_2, we have air-oxidized ReS_2 crystals (80° C for several hours) which leads to a formation of Re_2O_7. This is confirmed by the photoelectronspectra of the air-oxidized ReS_2 (see above). The (photo)electrochemical characteristics of these crystals are the same as for the electrochemically oxidized ReS_2.

The maximal photocurrent in such a cascade system (ReS_2/Re_2O_7 heterojunction) can be increased at AM1 from 34 mA cm^{-2} (single junction, E_G = 1.33 eV to 41 mA cm^{-2} (E_G = 1.33 and 2.6 eV) [17]. Of course, this rise is too modest to provide an explanation for the observed amplification of the photocurrent by 10 to 140 times. We prefer to assume that surface states in the ReS_2 single junction constitute recombination centres at the surface which do not allow a sufficiently high quantum efficiency. By forming the ReS_2/Re_2O_7 heterojunction the charge carriers produced in the sulphide cannot reach the electrode/electrolyte interface anymore. Consequently the quantum efficiency of ReS_2 rises (see Fig. 9).

Altogether, the amplification of the photocurrent may depend on:

- reduction of reflection from 40% [25] to 0–5% (max. factor 1.6)
- change from a single to a cascade system (factor 41/34)
- elimination of recombination centres by the formation of a heterojunction (main factor)

At the end of this photocurrent amplification (phase I in Fig. 5) $I_{ph} = I_{ph}^S$ is achieved. In phase II no further change of I_{ph} is noted. We thus consider phase I as the stabilization phase. Immediately after stabilization (point A), the cyclic voltamograms (Fig. 3) indicate two further corresponding peaks, which are the result of a reversible reaction with an E^0 (surface reaction) of +0.32 V with respect to SCE at pH 7. If it is considered that Re_2O_7 dissolves easily in aqueous sol-

utions to yield ReO_4^-, a possible reaction may be

$$ReO_4^- + 2H^+ + e^- \longleftrightarrow ReO_3\,(ad) + H_2O \quad (1)$$

In the initial stage of phase II (Fig. 5) the ReO_4^- concentration increases with each cycle and thus the height of the E^0 related peaks rises accordingly (see Fig. 3). Since the appearance of the two additional peaks correlates exactly with the end of the stabilization phase, it is supposed that the maximal photocurrent is limited by a certain layer thickness of Re_2O_7. On the other hand this result indicates that during the stabilization (phase I, no ReO_4^- related peaks) the Re_2O_7 formed does not dissolve immediately, which is even more important.

According to our results the material corrodes via the process $ReS_2 \rightarrow (ReO_xS_y) \rightarrow Re_2O_7 \rightarrow ReO_4^-$ (Fig. 5, phase III); ReO_xS_y indicates that the transformation from sulphide to oxide does not necessarily proceed in one step. Simultaneously, sulphur is oxidized to sulphate, as indicated by the XPS measurements (see Fig. 8). Altogether the following corrosion-reaction is suggested:

$$2ReS_2 + 38h^+ + 23H_2O \longrightarrow Re_2O_7(s) + 4H_2SO_4 + 38H^+ \quad (2)$$

followed by

$$Re_2O_7(s) + H_2O \longrightarrow 2HReO_4(sol.) \quad (3)$$

where h^+ is a light-created hole.

An oxidation of ReS_2 to Re_2O_7 in a N_2-rinsed solution is only possible if minority charge carriers are produced in ReS_2 and H_2O or OH^-, or OH radicals simultaneously reach the interface ReS_2/electrolyte. The creation of charge carriers in ReS_2 poses no problems, since photons with an energy < 2.6 eV penetrate the oxide layer. But the oxygen transport does; in this connection it is useful to remember that Re_2O_7 occurs also in a layer structure (Fig. 1b) [11] and that ReS_2 [26] as well as Re_2O_7 [27] allow intercalations. For this reason the following explanation seems to be promising. The influence of an anodic load provokes a solid state transformation in ReS_2 where OH is intercalated and ReS_2 is oxidized to Re_2O_7 (and to sulphate) by means of light-created holes. However, the structure of the layer does not change radically. OH^- can be discharged at the ReS_2 layers, to be intercalated in the layers (see Fig. 9). After a certain migration, it binds with rhenium or oxidizes the sulphur by means of light-created holes. The sulphur as a ligand is soon displaced by oxygen. The oxygen builds bridges between rhenium centres of various layers, providing the possibility that ReS_2 can be oxidized to Re_2O_7. These processes are accompanied by a parallel hydrogen emigration (see Fig. 9). Thus, we have to explain the process of corrosion with small dips which allow intercalations in deeper layers. These dips become microscopically visible as corrosion progresses. This mechanism is illustrated in Fig. 9. However, it must be considered that no direct experimental results are available to give particular information about the intermediate neutral sulphur species. In this context we would like to point out that similar effects of transformation could be observed in different sulphide materials, for example in ZrS_3 [28].

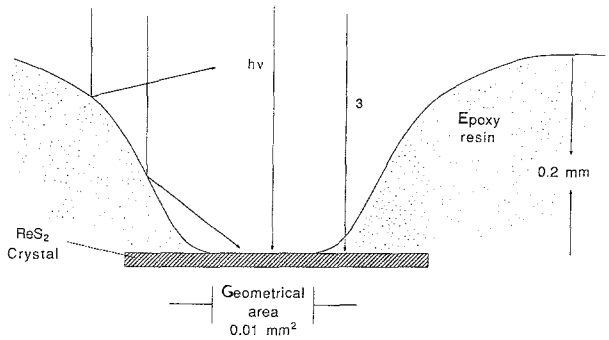

Fig. 10. Schematic view of how the insulation operates as collector at very small crystals.

Phase III in Fig. 5 shows the corrosion of ReS_2 due to the current flowing. The production of shunts by rupturing at the interstructural dips is indicated by an increase of the dark current and a simultaneous decrease of I_{ph}.

In the presence of O_2, the reaction in K_2SO_4 is supposed to proceed at the working electrode as follows:

$$2(x + y)ReS_2 + 38yh^+ + \tfrac{19}{2}xO_2 + 23yH_2O + 4xH_2O \longrightarrow (x + y)Re_2O_7 + 4(x + y)H_2SO_4 + 38yH^+ \quad (4)$$

where x and y depend on the kinetic constants of these parallel reactions; h^+ is a light-created hole.

The fact that in O_2 saturated solutions I_{ph}^S is already reached after $1\,C\,cm^{-2}$ instead of $50\,C\,cm^{-2}$ clearly shows the predominance of the oxidation by molecular oxygen as compared with the electrochemical oxidation ($x \gg y$ in the above equation). This is not surprising, since it is known that, in a purely chemical process, Re-compounds can be easily oxidized to rhenium of oxidation state VII by oxygen in water [24].

The stabilization effect is most evident in K_2SO_4 and KCl: in other electrolytes there is no oxide formation because the redox potential, to which the quasi-Fermi level of the holes is pinned, apparently, is too negative (Fig. 9). Considering this, it is understandable why there is a comparatively low current flowing in 1 M KI: only I_2 is formed, without corrosion. In KCl, we observe the formation of Cl_2 (gas bubbles appear and the insulation is impaired) besides the oxide formation (corrosion after ~ 16 h). This parallel reaction is easy to understand, since the thermodynamic corrosion potential ${}_pE_{corr}$ for the above mentioned reaction is situated at $+0.32$ V with respect to SCE at pH 7 (Fig. 9).

When an electrode is initially stabilized in 0.5 M K_2SO_4 and subsequently measured in KI, current–voltage curves appear as illustrated in Fig. 5. Besides the obvious photocurrent amplification there is no longer a steep rise of the dark current, that is more

Table 1. Correlation between the size of the crystals and the photocurrent after stabilization.

Size (mm^2)	*I_{Ph}^{Sa} at 1.5 V ($mA\,cm^{-2}$)*
0.53	22
0.19	30
0.06	55
0.03	63
< 0.01	> 120

positive than 0.6 V. An explanation for this appearance might be that the oxide impedes the formation of a rhenium–iodide complex, usually proceeding without light. After less than one minute the characteristic changes back to the initial situation: steep rise from 0.6 V on the smaller I_{ph}. This relatively quick dissolution of the oxide may be due to the fact that in KI ReS_2 cannot be further oxidized; instead a rhenium–iodide complex develops, leading to the destruction of the heterojunction.

5.1. *Collector effect*

The I_{ph}^{S}-values in Table 1 (particularly the last) are surprising since theoretically, under conditions of AM1 and having a single junction (E_G = 1.33 eV) a photocurrent of maximally 34 mA cm^{-2} can flow, and having a cascade system (1.33 and 2.6 eV) maximally 41 mA cm^{-2} [17]. The quantum efficiency would thus be ~3 which, of course, is impossible. The only explanation seems to be that the effective surface is larger than the optically measured geometric surface used for the ratio I_{ph} cm^{-2}.

Concerning the crystals investigated, such an enhancement can only be obtained by collecting light, i.e., the smaller the crystal, the higher the ratio between the height of the insulation and diameter of the crystal. The insulation has an effect upon the light similar to that of a (Winston) collector [29] (Fig. 10); the latter can increase the light intensity by maximally 6–fold. The smaller the crystals, the higher the above mentioned ratio, the more efficiently the insulation operates as a collector and, consequently, the higher is the effective increase of light intensity. This is clearly reflected by Table 1.

Give a collector which operates near optimum, the ratio between the effective and incident light intensity (I_e/I_i) can be estimated to be 3–4. These reduce the real measured photocurrent density of 120 mA cm^{-2} (for the smallest crystals, see Table 1) to 30–40 mA cm^{-2} at AM1 which is theoretically feasible. For very small crystals we have also to take into account that the edge of the insulation is often not in best contact with the crystal and electrolyte can flow under the insulation. Moreover, near the edge of the insulation we can find areas of very thin insulation which are transparent to a certain amount of light (see Fig. 10, arrow 3). of course, effects like this are only important when using very small crystals.

Acknowledgement

The authors would like to thank Dr. S. Fiechter for help with the synthesis, Dr. W. Jaegermann for making the XPS-experiments and to Dr. W. Hofmann for making the SEM-pictures. B. Schubert would like to thank the Fonds der Chemischen Industrie for financial support.

References

[1] W. H. Davenport, V. Kollonitsch and C. H. Kline, *Ind. Eng. Chem.* **60** (1968) 10.
[2] M. A. Ryashentseva and Kh. M. Minachev, *Russ. Chem. Rev.* **38** (1969) 944.
[3] C. Bolivar, H. Charcosset, R. Frety, M. Primet, L. Tournayan, C. Betizeau, G. Leclercq and R. Maurel, *J. Cat.* **39** (1975) 249.
[4] J. Horkans and M. W. Shafer, *J. Electrochem. Soc.* **124** (1977) 1202.
[5] J. V. Marzik, R. Kershaw, K. Dwight and A. Wold, *J. Solid State Chem.* **51** (1984) 170.
[6] B. L. Wheeler, J. K. Leland and A. J. Bard, *J. Electrochem. Soc.* **133** (1986) 358.
[7] Landolt-Börnstein III/17 g, (edited by K. H. Hellwege and O. Madelung), Springer, Verlag, Berlin (1984).
[8] B. Schubert and H. Tributsch, publication pending.
[9] J. C. Wildervanck and F. Jellinek, *J. Less Common Metals* **24** (1971) 73.
[10] H. E. Swanson and R. K. Euyat, Natl. Bur. Std. (U.S.) Circ. 539 II, (1953) 13.
[11] B. Krebs, A. Müller and H. H. Beyer, *Inorg. Chem.* **8** (1968) 436.
[12] L. Gmelins's, 'Handbuch der anorganischen Chemie', 8 Auflage, (edited by Deutsche Chemische Gesellschaft), Verlag Chemie Weinheim, Berlin (1941); System-Nr. 70, p. 94.
[13] H. Frederiksson, B. Kasemo and I. Marklund, *Thin Solid Films* **8** (1971) 61.
[14] R. Juza and W. Biltz, *Z. Electrochem.* **37** (1931) 498.
[15] J. Sodi and J. F. Elliot, *Trans. Met. Soc. AIME* **242** (1968) 2143.
[16] ASTM Datenkarte Nr. JCP55, Swarthmore PA (1978).
[17] H. J. Hovel, in 'Semiconductors and Semimetals', 11, Solar cells, Academic Press, London (1975) p. 38.
[18] A. Cimino, B. A. De Angelis, D. Gazzoli and M. Valigi, *Z. Anorg. Allg. Chem.* **460** (1980) 86.
[19] XPS-Handbood, (edited by C. D. Wagner, W. M. Riggs, L. E. Davis, J. F. Moulder and G. E. Mullenberg), Perkin-Elmer Corp. (1978).
[20] G. Rouschias, *Chem. Rev.* **74** (1974) 531.
[21] S. Tribalat, D. Delafosse and C. Piolet, *C. R. Acad. Sci.* **261** (1965) 1008.
[22] V. A. Petrovich, L. V. Tabulina and S. I. Arzhanov, *Khim. Khim. Tekhol. Minsk.* **19** (1984) 47.
[23] J. A. Wilson and A. D. Yoffe, *Adv. Phys.* **18** (1969) 193.
[24] 'Encyclopedia of Electrochemistry of the Elements', Vol. 2 (edited by A. J. Bard) Marcel Dekker, New York (1974) p. 125 ff.
[25] V. V. Sobolev, V. I. Donetskikh, A. A. Opalovskii, V. E. Fedorov, E. U. Lobkov and A. P. Mazhara, *Soviet Physics-Semiconductors* **5** (1971) 909.
[26] W. Rüdorff, *Chimia* **19** (1965) 489.
[27] D. W. Murphy, P. A. Christian, J. N. Carides and F. J. DiSalvo, 'Fast Ion Transp. Solids: Electrodes Electrolytes', Proc. Int. Conf. (1979) p. 137.
[28] O. Gorochov, A. Katty, N. LeNagard, C. Levy-Clement, A. Redon and H. Tributsch, *J. Electrochem. Soc.* **130** (1983) 1301.
[29] R. Winston, *Appl. Optics* **15** (1976) 292.
[30] N. W. Alcock and A. Kjekshus, *Acta Chem. Scand.* **19** (1965) 79.